Rare b decays and Observation of B_c^+ Mesons at Tevatron

Jun-ichi SUZUKI
Institute of Physics, University of Tsukuba, 1-1-1 Tennoudai, Tsukuba Ibaraki 305, Japan [a]
(for the CDF and DØ COLLABORATIONS)

We report the results of the search for flavor-changing neutral current (FCNC) decays $b \to s\mu^+\mu^-$ and the observation of B_c^+ mesons at Tevatron.

1 Introduction

We present the results from searches for flavor-changing neutral-current (FCNC) decays and the observation of B_c^+ mesons at Tevatron.

The FCNC decays $b \to s\ell^+\ell^-$ are forbidden at tree level. They can proceed through the higher order diagrams, such as penguin and box diagrams with one loop. These diagrams are sensitive to CKM-matrix element V_{ts}, and are also sensitive to new physics such as charged Higgs bosons, new gauge bosons or supersymmetric particles which can contribute through the loop. The Standard Model prediction [1] for the branching fraction of $b \to s\ell^+\ell^-$ is $\mathcal{O}(10^{-6})$. The lepton pair can be resonant, for example, J/ψ and $\psi(2S)$. They are not distinguishable from the internal spectator decay, $b \to cW^- \to c\bar{c}s$. So we search for non-resonant part of the dilepton mass spectrum. CDF and DØ search for the FCNC decays of $b \to s\mu^+\mu^-$ modes which can be triggered easily at a hadron collider due to their dimuon signature.

The B_c^+ meson is a bound state of a $\bar{b}$ quark and a c quark, and is expected to be the heaviest meson consisting of different flavored quarks. The Standard Model predicts an existence of the B_c^+ meson. The top quark is so heavy that it cannot form a meson. Therefore, the B_c^+ meson is the heaviest meson consisting of different flavored quarks. The B_c^+ production rate is expected to be 10^{-3} times $b\bar{b}$ production rate, according to perturbative QCD calculations of α_s^4 order [2]. The mass of the $\bar{b}c$ ground state is expected to be 6.258±0.020 GeV/c^2 within the framework of nonrelativistic QCD potential models [3]. Since the B_c^+ meson has non-zero flavor, it decays only via weak interaction. The predictions for the B_c^+ lifetimes lie in a wide range: $0.3 < \tau < 1.4$ ps, depending on the modeling of binding energy effects [4]. LEP [5] and CDF [6] have set upper limits on the production rate for for B_c^+ mesons, but could not find them previously.

2 Search for the flavor-changing neutral-current decays $b \to s\mu^+\mu^-$

2.1 Search for Inclusive FCNC decays $b \to X_s\mu^+\mu^-$ at DØ

DØ searches for the inclusive FCNC decays $b \to X_s\mu^+\mu^-$ using 50 pb^{-1} of data [7]. Dimuon candidates are required to have an oppositely charged muon pair with the invariant mass $m(\mu^+\mu^-)$

[a] Present Address: High Energy Accelerator Research Organization, 1-1 Oho, Tsukuba Ibaraki 305-0801, Japan

< 7 GeV/c^2, transverse momentum $p_T(\mu^+\mu^-) > 5$ GeV/c and pseudo-rapidity $|\eta(\mu^+\mu^-)| < 0.6$. Both muons are also required to have $p_T(\mu^\pm) > 3.5$ GeV/c and $|\eta(\mu^\pm)| < 1.0$. The dimuon invariant mass distribution for these candidates is shown in Fig. 1.

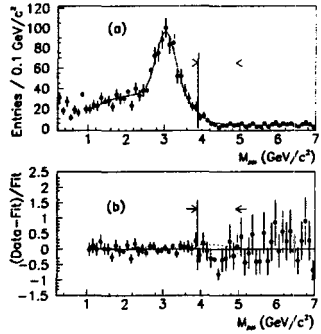

Figure 1: (a) Dimuon invariant mass spectrum. The solid curve is the fit result. (b)Data - Fit/Data. The dashed curve corresponds to an upper limit of $b \to X_s\mu^+\mu^-$ contribution at 90% confidence level from the fit.

The dimuon invariant mass distribution is fitted to a sum of the following sources in the mass window $3.9 < m(\mu^+\mu^-) < 4.9$ GeV/c^2:(1) J/ψ and $\psi(2S)$ signal, (2) double semileptonic decays of $b\bar{b}$ and $c\bar{c}$ events, (3) a sequential semileptonic decay of b hadron, (4) one muon from a true semileptonic decay of b or c quark and the other from K^+ or π^+ decay-in-flight and (5) dimuon produced through the Drell-Yan process. The fit result is shown in Fig. 1 (a) and (Data - Fit)/ Fit is shown in Fig. 1 (b). They observe 56 events in the mass window, while 68 ± 2(stat.)± 4(syst.) events are obtained from the fit. There is no evidence of an excess for $b \to X_s\mu^+\mu^-$ events. An upper limit on the branching fraction of the $b \to X_s\mu^+\mu^-$ decay is given as $\mathcal{B}(b \to X_s\mu^+\mu^-) < 3.2 \times 10^{-4}$ at 90% confidence level. The Standard Model prediction[1] for the branching fraction is $(5.7 \pm 1.2) \times 10^{-6}$ and the best limit[8] obtained by CLEO is $\mathcal{B}(b \to X_s\mu^+\mu^-) < 5.8 \times 10^{-5}$ [b].

2.2 *Search for Exclusive FCNC decays $B \to K^{(*)}\mu^+\mu^-$ in CDF*

The search for the exclusive FCNC decays, $B^+ \to K^+\mu^+\mu^-$ and $B^0 \to K^{*0}\mu^+\mu^-$ ($K^{*0} \to K^+\pi^-$) have been performed using 90 pb^{-1} of data at CDF. The full reconstruction of the B meson at CDF reduces backgrounds significantly. The $K^{(*)}\mu^+\mu^-$ candidates must satisfy the following selection criteria: $p_T(K^{(*)}\mu^+\mu^-) > 6$ GeV/c, $|\eta(K^{(*)}\mu^+\mu^-)| < 1$, transverse decay length $L_{xy} > 400$ μm and isolation $I > 0.6$, where I is defined as the p_T of the $K^{(*)}\mu^+\mu^-$ candidates divided by the scalar sum of all charged tracks within a cone $\sqrt{\eta^2 + \phi^2} < 1$, including $p_T(K^{(*)}\mu^+\mu^-)$. To remove backgrounds further, the impact parameter significance for each track is required to be greater than 2. The resonant part of the dimuon mass, *i.e.* ± 200 MeV/c^2 (± 100 MeV/c^2) around the world average mass of J/ψ ($\psi(2S)$), is excluded in these searches.

The $K^+\mu^+\mu^-$ invariant mass distribution is shown in Fig. 2. The top plot in Fig. 2 is the mass distribution for the resonant dimuon events and the bottom one is for the non-resonant ones. The $K^{*0}\mu^+\mu^-$ invariant mass distribution for the resonant decays and the non-resonant decays are shown in Fig. 2. The $K^{(*)}\mu^+\mu^-$ signal region is defined as $|m(K^{(*)}\mu^+\mu^-) - m(B)| < 50$ MeV/c^2, where $m(B)$ is the world average B meson mass. The high mass region $100 <$

[b] CLEO also obtained the 90% C.L. limit for the branching fraction, $\mathcal{B}(b \to X_s e^+e^-) < 5.7 \times 10^{-5}$. Combining the dielectron and dimuon decay modes, they found $\mathcal{B}(b \to X_s\ell^+\ell^-) < 4.2 \times 10^{-5}$.

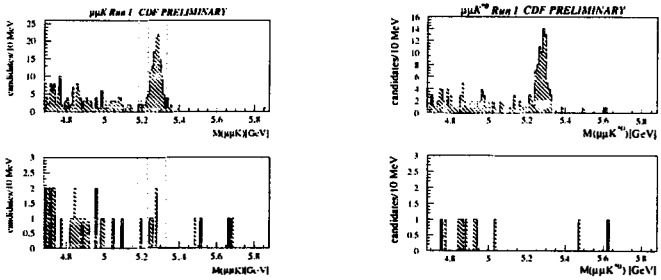

Figure 2: $K^{(*)}\mu^+\mu^-$ invariant mass distribution. Left: for $B^+ \to K^+\mu^+\mu^-$ resonant decay (top) and non-resonant decay (bottom). Right: for $B^0 \to K^{0*}\mu^+\mu^-$ resonant decay (top) and non-resonant decay (bottom).

$m(K^{(*)}\mu^+\mu^-) - m(B) < 600$ MeV/c^2 is used to define the background region, since events in the mass region below $m(B)$ can include $B \to J/\psi X$ decays. For the resonant decays (Fig. 2 top), we find a significant peak in the signal region, while few events are in the background region. For the non-resonant decays (Fig. 2 bottoms), 4 candidates and 4 background events are found in the $B^+ \to K^+\mu^+\mu^-$ mode. No candidate and 2 background events are found in the B^0 $K^{*0}\mu^+\mu^-$ mode. From the Standard Model prediction for the branching fractions, we expect 0.6 events of the $B^0 \to K^{*0}\mu^+\mu^-$ decays in the signal region using the number of the $B^0 \to K^{*0}\psi$ decays for normalization.

We see no excess due to the FCNC decay in both modes. Without background subtraction, we obtain the 90% C.L. upper limit for the branching fractions to be $\mathcal{B}(B^+ \to K^+\mu^+\mu^-) < 5.4 \times 10^{-6}$ and $\mathcal{B}(B^0 \to K^{*0}\mu^+\mu^-) < 4.1 \times 10^{-6}$, while the Standard Model predictions[1] are $(0.40 \pm 0.14) \times 10^{-6}$ and $(1.5 \pm 0.5) \times 10^{-6}$, respectively. These are the most stringent limits so fat achieved for these decay modes.

3 Observation of B_c^+ Mesons in CDF

3.1 Event Selection and Background Estimation

CDF searches for $B_c^+ \to J/\psi\ell^+X$ ($\ell = e$ or μ), where $J/\psi \to \mu^+\mu^-$, using 110 pb^{-1} of data.[9] We select $J/\psi \to \mu^+\mu^-$ events where both muon tracks are reconstructed in the CDF silicon vertex detector (SVX). We find 196,000 $J/\psi \to \mu^+\mu^-$ events and apply the dimuon mass window cut $|m(\mu^+\mu^-) - m(J/\psi)| < 50$ MeV/c^2, where $m(J/\psi)$ is the world average J/ψ mass. In the dimuon mass window, we search for a third lepton with $p_T(e) > 2$ GeV/c or with $p_T(\mu) > 3$ GeV/c, where the third lepton and J/ψ are in the same hemisphere. The three leptons (μ^+, μ^-, ℓ) are required to form a good common vertex. Since there is missing momentum due to the neutrino in the semileptonic decay mode, we cannot fully reconstruct the B_c^+ momentum and mass. From the Monte Carlo simulation, the invariant mass of J/ψ-lepton combination falls in the range 4 GeV/c^2 to 6 GeV/c^2 for B_c^+ signals. Therefore, the signal region is defined as $4 < m(J/\psi\ell) < 6$ GeV/c^2. To remove prompt J/ψ events, we apply the pseudo-proper decay length cut, $ct^* \equiv \frac{m(J/\psi\ell)}{p_T(J/\psi\ell)} L_{xy} > 60$ μm, where L_{xy} is the transverse decay length. Fig. 3 (a) shows the J/ψ + 'track' mass distribution, where 'track' satisfies only the lepton fiducial requirements without lepton identification requirements. These distributions are used for estimating the various backgrounds. Figs. 3 (b) show the $J/\psi + \ell$ mass distribution. We find 19 $J/\psi + e$ events and 12 $J/\psi + \mu$ events in the mass range $4 < m(J/\psi\ell) < 6$ GeV/c^2.

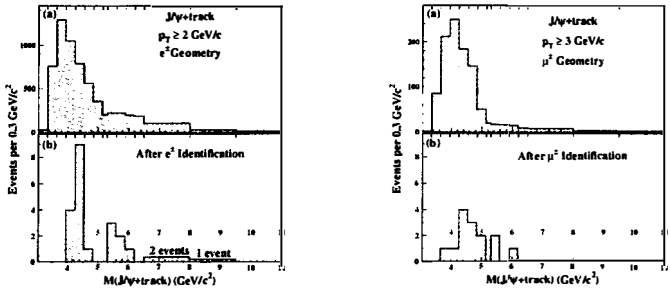

Figure 3: The mass distribution for J/ψ + track (a), where 'track' just satisfies the fiducial requirements, and for $J/\psi + \ell$ (b). Left: $J/\psi + e$. Right: $J/\psi + \mu$.

Table 1: Summary of Counting Experiments

	$4.0 < M(J\psi\ell) < 6.0$ GeV/c^2	
	J/ψ e results	J/ψ μ results
Misidentified leptons		
Fake Electrons	$2.6 \pm 0.05 \pm 0.3$	
Conversions	$1.2 \pm 0.8 \pm 0.4$	
Punch-through		$0.88 \pm 0.13 \pm 0.33$
Decay-in-flight		$5.5 \pm 0.5 \pm 1.3$
$b\bar{b}$ bkg.	1.2 ± 0.5	0.7 ± 0.3
Total Background	5.0 ± 1.1	7.1 ± 1.5
Events observed in data	19	12
Net Signal	14.0	4.9
Combined	18.9	
$P_{Counting}$(Null)	2.1×10^{-5}	0.084

We identify and estimate the following background sources: For the electron mode, the dominant background sources are (i) fake electron background due to hadrons (π or K) misidentified as electrons, (ii) residual conversion background due to electrons not found by the conversion electron finding algorithm, and (iii) $b\bar{b}$ background due to events in which the J/ψ comes from one $\bar{b}$ and the electron from the other b. The dominant backgrounds for the muon mode are (i) punch-through background due to hadrons that traverse without interacting in the calorimeter and hit a muon chamber, (ii) decay-in-flight background due to hadrons that decay into muons, and (iii) $b\bar{b}$ background. The numbers of these backgrounds and the results of counting experiment are summarized in Table 1. We see some excesses in both modes and will discuss a statistical significance of the excesses in the next section.

3.2 Statistical Significance of Signal

To test a statistical significance of the apparent excess, we perform the mass shape analysis. We fit the observed $J/\psi\ell$ mass distribution in the range from 3.35 to 11.0 GeV/c^2 to a sum of B_c^+ signal and the backgrounds using a binned likelihood method. The signal shape is obtained from Monte Carlo simulation for the $B_c^+ \to J/\psi\ell^+\nu$ decay, and each background shape discussed in the previous section is obtained using the CDF real data and Monte Carlo simulation. In the

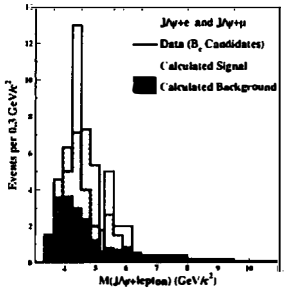

Figure 4: $J/\psi\ell$ mass distribution with the fit result.

fit, only the number of B_c signals is an unconstrained parameter. Other parameters, such as the expected fraction of two modes, the number of backgrounds and the background shapes, are constrained to the estimated ones within their uncertainties. The $J/\psi\ell$ mass distribution is shown together with the fit results in Fig. 4. From the fit, we obtain the number of B_c^+ signals $N(B_c^+)$ to be $20.4^{+6.2}_{-5.5}$.

We test a null hypothesis as follows. We allow the number of events for each source of background to fluctuate according to its uncertainty, and we generate a combined mass distribution using the known shapes of the backgrounds. We then fit these Monte Carlo mass distributions to a sum of B_c^+ signal and background, exactly as done for real data. For 351,900 trials for this process, we estimate the number of trials where $N(B_c^+)$ is greater than 20.4 to be 0.22. Thus we find the probability that a statistical fluctuation in the background can explain the excess in the data to be 6.3×10^{-7}; this corresponds to 4.8 standard deviations in significance. In the next section, we measure the basic properties, such as mass, lifetime and cross section ratio of B_c^+ mesons, assuming that the observed excesses are due to the existence of the B_c^+ meson.

3.3 Measurement of the B_c^+ properties Mass, Lifetime and Cross section Ratio

The B_c^+ meson mass is measured using the same fitting technique as in the preceding section. We fit the $m(J/\psi\ell)$ distribution to a sum of B_c^+ signal and the backgrounds varying the assumed B_c^+ mass from 5.52 to 7.52 GeV/c^2. The relative log-likelihood $\xi_m = -2\ln\left(\frac{\mathcal{L}(m)}{\mathcal{L}(m=6.40)}\right)$ at each assumed B_c^+ mass is shown in Fig. 5. From the minimum ξ_m, the B_c^+ mass is determined to be $6.40 \pm 0.39(\text{stat.}) \pm 0.13(\text{syst.})$ GeV/c^2.

We loosened the $ct^* > 60$ μm cut to the $ct^* > -100$ μm cut in order to measure the B_C^+ lifetime using the entire ct^* distribution. Since we cannot fully reconstruct the B_c^+ mass and momentum event by event due to the missing momentum, we correct for the missing momentum using Monte Carlo simulation. The relation between ct^* and proper decay length ct is given by $ct^* = \frac{ct}{K}$, where $K = \frac{m(B_c^+)}{m(J/\psi\ell^+)} \times \frac{p_T(J/\psi\ell^+)}{p_T(B_c^+)}$. We obtain the K distribution from the Monte Carlo simulation and convolute an exponential tail with the K distribution in the signal shape. We also obtain the ct^* distribution for backgrounds discussed in Section 3.1. Then we fit the observed ct^* distribution to a sum of B_c^+ signal and backgrounds, using an unbinned likelihood method. The ct^* distribution is shown in Fig. 5 together with the fit result. The B_c^+ lifetime is measured to be $0.46^{+0.18}_{-0.16}(\text{stat.}) \pm 0.03(\text{syst.})$ ps.

We measure the cross section ratio $\mathcal{R}$ of $\sigma(B_c^+)\mathcal{B}(B_c^+ \to J/\psi\ell^+\nu)$ to $\sigma(B_u^+)\mathcal{B}(B_u^+ \to J/\psi K^+)$. The event topology for the $B_u^+ \to J/\psi K^+$ is very similar to that for the B_c^+ semilep-

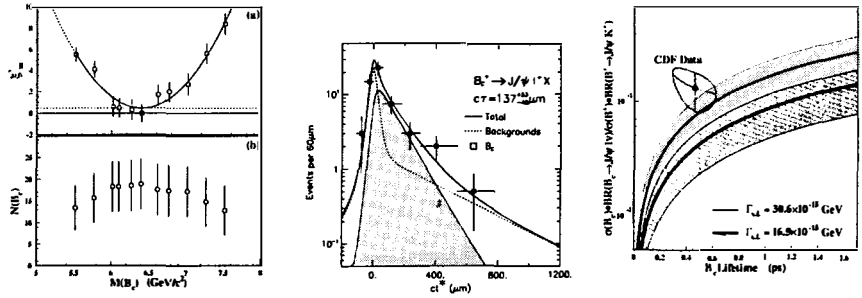

Figure 5: Left: (a) ξ_m^2 and (b) $N(B_c^+)$ as a function of an assumed B_c^+ mass. Middle: ct^* distribution with the fit result. Right: $\sigma\mathcal{B}$ ratio as a function of the observed B_c^+ lifetime. The shaded regions are theoretical predictions with the two different partial widths.

tonic decay. Therefore, many systematic uncertainties are canceled in the ratio. The ratio $\mathcal{R}$ is measured to be $0.132^{+0.041}_{-0.037}$(stat.)± 0.031(syst.)$^{+0.032}_{-0.020}$(lifetime) and is plotted with the B_c^+ lifetime in Fig. 5. It is consistent with the theoretical prediction.

4 Conclusions

In the Tevatron experiments, the searches for the FCNC decays $b \to s\mu^+\mu^-$ were performed. The FCNC decays have not been observed yet.

The CDF experiment observed the B_c^+ meson through the $B_c^+ \to J/\psi\ell^+X$ mode. We find $20.4^{+6.2}_{-5.5}$ B_c^+ signals from the the $J/\psi\ell$ mass fit. A fit without B_c^+ contribution is rejected at the level of 4.8 standard deviations. Then we measured the B_c^+ properties: (1) mass: 6.40 ± 0.39(stat.)± 0.13(syst.) GeV/c^2; (2) lifetime: $0.46^{+0.18}_{-0.16}$(stat.)± 0.03(syst.) ps, and (3) cross section ratio $\mathcal{R}$: $0.132^{+0.041}_{-0.037}$(stat.)± 0.031(syst.)$^{+0.032}_{-0.020}$(lifetime).

References

1. A. Ali, DESY 97-019, hep-ph/97022312.
2. C.H. Chang, Y.Q. Chen and R.J. Oakes, *Phys. Rev.* D **54**, 4344 (1996); M. Lusignoli, M. Masetti and S. Petrarca, *Phys. Lett.* B **266**, 142 (1991).
3. E.J. Eichten and C. Quigg, *Phys. Rev.* D **49**, 5484 (1994).
4. C. Quigg, FERMILAB-CONF-93/265-T; I.I. Bigi, *Phys. Lett.* B **371**, 105 (1996); M. Beneke and G. Buchalla, *Phys. Rev.* D **49**, 4991 (1996).
5. R. Barate *et al*, *Phys. Lett.* B **402**, 213 (1997); P. Abreu *et al*, *Phys. Lett.* B **398**, 207 (1997); G. Alexaunder *et al*, *Phys. Lett.* B **420**, 157 (1998).
6. F. Abe *et al*, *Phys. Rev. Lett.* **77**, 5176 (1996).
7. B. Abbot *et al*, *Phys. Lett.* B **423**, 419 (1998).
8. CLEO Collaboration, CLNS 97/1514, hep-ex/971003.
9. F. Abe *et al*, FERMILAB-PUB-98-121-E, submitted to *Phys. Rev.* D.